Journal of Solid State Chemistry 184 (2011) 2724–2730

Contents lists available at SciVerse ScienceDirect

Journal of Solid State Chemistry

journal homepage: www.elsevier.com/locate/jssc

Influence of silver-decorated multi-walled carbon nanotubes on electrochemical performance of polyaniline-based electrodes

Ki-Seok Kim, Soo-Jin Park*

Department of Chemistry, Inha University, Incheon 402-751, Republic of Korea

ARTICLE INFO

Article history:
Received 10 April 2011
Received in revised form
20 July 2011
Accepted 10 August 2011
Available online 16 August 2011

Keywords:
Multi-walled carbon nanotubes
Polyaniline
Silver nanoparticles
Electrochemical properties

ABSTRACT

In this work, silver (Ag) nanoparticles were deposited on multi-walled carbon nanotubes (MWNTs) by chemical reduction while Ag-decorated MWNTs (Ag-MWNTs)/polyaniline (PANI) composites were prepared by oxidation polymerization. The effect of the Ag incorporated into the interface of the composites on the electrochemical performance of the MWNTs/PANI was investigated. It was found that highly dispersed Ag nanoparticles were deposited onto the MWNTs, and the Ag-MWNTs were successfully coated by PANI. According to cyclic voltammograms, the Ag-MWNTs/PANI exhibited significantly increased electrochemical performances compared to MWNTs/PANI and the highest specific capacitance obtained of MWNTs/PANI and 0.15 M Ag-MWNTs/PANI was 162 F/g and 205 F/g, respectively. This indicated that Ag nanoparticles that were deposited onto the MWNTs caused an enhanced electrochemical performance of the MWNTs/PANI due to their high electric conductivity, which resulted in an increase of the charge transfer between the MWNTs and PANI by a bridge effect.

1. Introduction

Carbon nanotubes (CNTs) are recognized as reinforcements for high performance and multifunctional composites because of their extraordinary mechanical strength and excellent electrical/thermal conductivity. Considerable achievements have been made in CNT-polymer composites and a remarkable enhancement in electrical and mechanical properties compared to those of monolithic polymers has been observed [1–4].

Among numerous conductive polymers, polyaniline (PANI) is considerably attractive because of easy synthesis, environmental stability, high and controllable conductivity, and its various applications, such as lightweight battery electrodes, energy storage devices, electromagnetic shielding devices, anticorrosion coatings, sensors, etc. Recently, CNTs/PANI composites have attracted much attention in studies to enhance electrical and mechanical properties over pure PANI [5–9]. Although CNTs/PANI are also widely studied as electrode materials for supercapacitors, the use of these individual materials in electrodes is limited by their drawbacks, such as the high cost of CNTs and weak mechanical properties and poor life of PANI. Therefore, PANI composites combined with CNTs will provide synergistic performance on the electronic and mechanical properties by the interaction of the two components [10,11].

For application of CNT/PANI as electrode materials, the functionality and process ability of the composites are key points. These properties are related to the dispersion of the CNTs and the interfacial adhesion between the CNTs and the PANI matrix. Various methods have obtained CNTs/PANI composites, such as solution mixing, direct mechanical mixing, and *in situ* or electrochemical polymerization, etc. [12,13].

Lately, metal doped PANI composites are also attractive materials as they combine the properties of low dimensional organic conductors and high surface area materials, and are currently of great research interest due to the numerous applications for PANI, as well as the unique optical and catalytic properties of metal nanoparticles. However, many studies have been performed on the effect of metal decoration on the electrochemical properties of MWNTs or MWNTs/PANI, whereas there has been limited work on the effect of metal incorporation between MWNTs and PANI on the electrochemical properties of MWNTs/PANI [14,15].

In the present work, multi-walled carbon nanotubes (MWNTs) are decorated by silver (Ag) nanoparticles, and the Ag-decorated MWNTs (Ag-MWNTs)/polyaniline (PANI) composites were prepared by oxidation polymerization of the corresponding aniline monomer in the presence of MWNTs in a solution. The effect of Ag incorporated between the components on the electrochemical properties of the MWNTs/PANI is discussed.

2. Experimental

2.1. Materials

Multi-walled carbon nanotubes (MWNTs) produced by chemical vapor deposition (CVD) process were obtained from Nanosolution

* Corresponding author. Fax: +82 32 860 8438.
E-mail address: sjpark@inha.ac.kr (S.-J. Park).

0022-4596/$ - see front matter © 2011 Elsevier Inc. All rights reserved.
doi:10.1016/j.jssc.2011.08.010

Co. (Korea). The properties of the MWNTs were as follows: purity > 95% (C: 96%), diameter 10–25 nm and length 25–50 μm. Aniline, silver nitrate, polyvinyl pyrrolidone (PVP), and ammonium persulfate (APS) were obtained from Aldrich. 3-amine propyltrimethoxysilane (APTMS) and hydrazine monohydrate was supplied from TCI and Sam Chum Chem. (Korea), respectively. The sulfuric acid, nitric acid, and all other organic solvents used in this study were of analytical grade and used without further purification.

2.2. Silver decoration on the MWNTs

One gram of MWNTs was acid-treated with 200 ml of a sulfuric acid and nitric acid mixture (3:1, v/v) under sonication for 2 h and was then reacted for 6 h at 80 °C with reflex under stirring. Acid-treated MWNTs (A-MWNTs) were washed using water until pH 7.0 was attained, after which the washed samples were filtered and dried at 100 °C.

Ag decorated MWNTs were prepared by the reducing reaction of silver ions using hydrazine. 0.1 g of A-MWNTs was suspended in 100 ml of 0.5 wt% PVP solution containing 0.5 M APTMS and stirred with ultrasonic treatment for 1 h. Before the reaction, 0.1 M HNO_3 was added to adjust the pH for weak acidic solution (pH = 6). Twenty milliliter of silver nitrate solution (0.05, 0.1, and 0.15 mol/L) was added to the MWNT solution within 30 min at 60 °C while the MWNT solution was stirred and then hydrazine was added to the mixture solution. This mixture was kept with stirring at room temperature for 24 h. Finally, Ag-MWNTs were obtained by filtration and washed with de-ionized water and acetone, and then and dried in a vacuum oven for 24 h. The preparation procedure of Ag decorated MWNTs is presented in Fig. 1 and named 0.05 Ag-MWNTs, 0.1 Ag-MWNTs, and 0.15 Ag-MWNTs.

2.3. Preparation of Ag-MWNTs/PANI

0.1 g of A-MWNTs (Ag-MWNTs) was dispersed in 100 ml of 1 M HCl solution with the assistance of ultrasonication for 1 h. Five milliliter of the aniline monomer was added to the MWNTs solution with constant stirring. Finally, 100 ml of 0.1 M APS solution was dropped in the above solution for 30 min to initiate the polymerization. The reaction was continued for 24 h at 0–5 °C. Then, the final product was washed using water and acetone. The washed powder was dried in a vacuum oven at 80 °C for 24 h. The scheme for the preparation of Ag-MWNTs/PANI is presented in Fig. 1.

2.4. Measurements

Ag-MWNTs were confirmed using transmission electron microscopy (TEM, JEOL FE-TEM 2006) and X-ray diffraction (XRD, Rigaku D/Max 2200 V) at 40 kv and 40 mA using Cu $K\alpha$ radiation. The XRD patterns were obtained in 2θ ranges between 5° and 70° at a scanning rate of 2°/min.

Infrared spectra of A-MWNTs, Ag-MWNTs, and Ag-MWNTs/PANI were confirmed with Fourier transform infrared spectrophotometer (FT-IR 4200, Jasco).

The thermal property of Ag-MWNTs, PANI, and Ag-MWNTs/PANI was measured using thermogravimetric analyses (TGA, DuPont TGA-2950 analyzer) from 30 to 850 °C at a heating rate of 10 °C/min in a nitrogen atmosphere.

The morphologies of Ag-MWNTs, PANI, and Ag-MWNTs/PANI were observed by scanning electron microscopy (SEM, S-4200, Hitachi).

Electrical conductivity of the Ag-MWNTs/PANI was measured at room temperature using a four probe digital multimeter

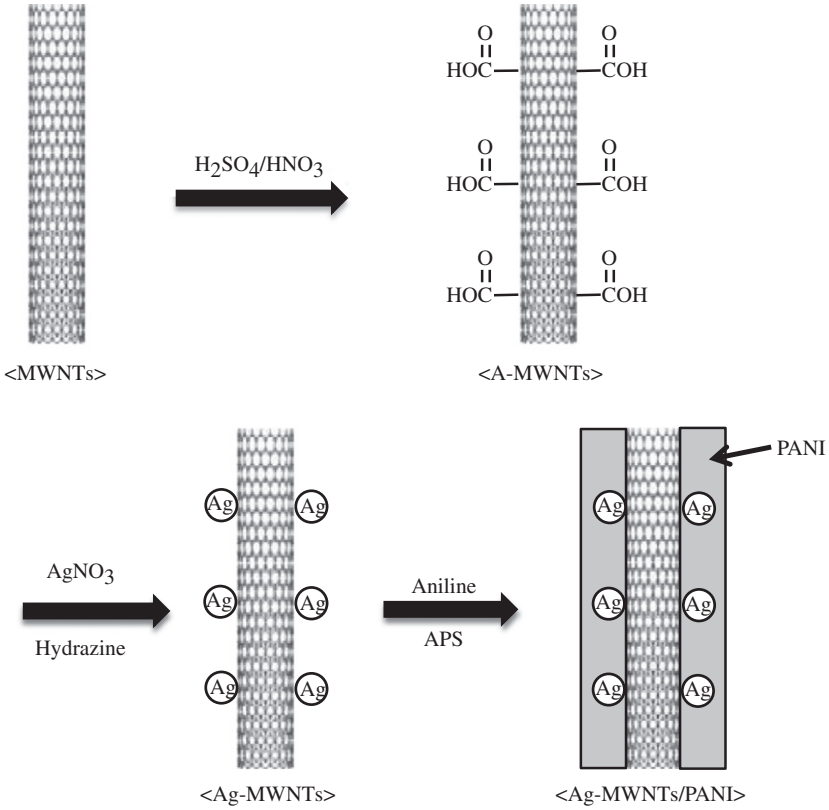

Fig. 1. Schematic diagram showing the preparation of Ag-MWNTs and Ag-MWNTs/PANI.

(MCP-T610, Mitsubishi Chem.). The powder was compacted as plate form and the specimen size was 0.5 mm × 10 mm × 30 mm.

The electrochemical properties of the MWNTs/PANI and Ag-MWNTs/PANI were characterized using a three-electrode electrochemical cell. The three-electrode cell consisted of a Pt wire as a counter electrode, an Ag/AgCl reference electrode, and a sample mixed with Nafion® polymer onto a glassy carbon electrode as a working electrode. Cyclic voltammetry measurements were carried out on an IviumStat instrument in 1.0 M sulfuric acid at a scan rate of 50 mV/s in a voltage range of −0.2 to 1.5 V.

3. Results and discussion

3.1. Characterization of Ag-MWNTs

Fig. 2(a) and (b) shows the TEM images of pristine MWNTs and Ag-MWNTs. From the TEM images, a pristine MWNT surface is clean without any Ag particles while the Ag-MWNTs show Ag nanoparticles decorated on the MWNT surface after chemical reduction [16,17]. The Ag nanoparticles are distributed on MWNTs without agglomeration, and their sizes range from 2 nm to 4 nm (separated Ag particles between MWNTs are due to the sonication for TEM sampling). This indicates that the oxygen-containing surface groups (carbonyl and hydroxyl groups) on A-MWNTs may function as anchoring sites for an Ag precursor to prevent the aggregation of the Ag nanoparticles, leading to the good dispersion of Ag nanoparticles on MWNTs [18]. A single peak of Ag onto MWNTs is also observed at the EDX spectrum, as shown in Fig. 1(c).

Fig. 3 shows the XRD patterns for the pristine MWNTs and Ag-MWNTs. The pristine MWNTs revealed reflections corresponding to the C(0 0 2) and C(1 0 0) planes of crystalline graphite-like materials at $2\theta = 26^\circ$ and 43°, respectively [19], whereas the Ag-MWNTs show those corresponding to three main crystallographic plans of Ag, namely, Ag(1 1 1), Ag(2 0 0), and Ag(2 2 0). These results indicate that Ag nanoparticles are successfully decorated onto the MWNTs by the chemical reduction method.

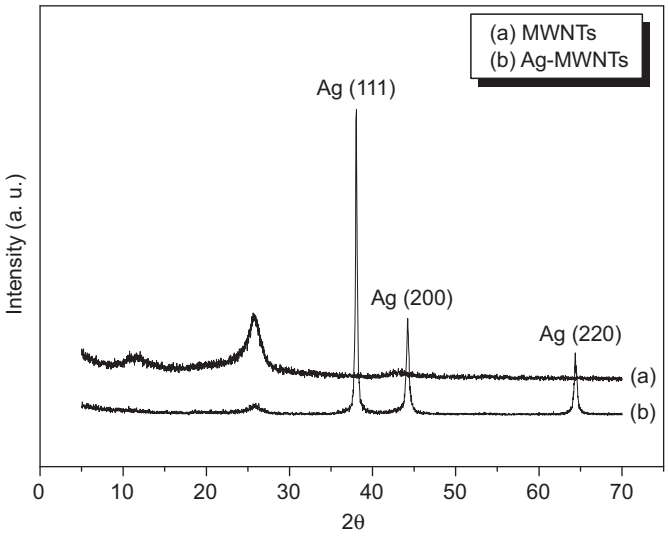

Fig. 3. XRD patterns of pristine MWNTs and Ag-MWNTs.

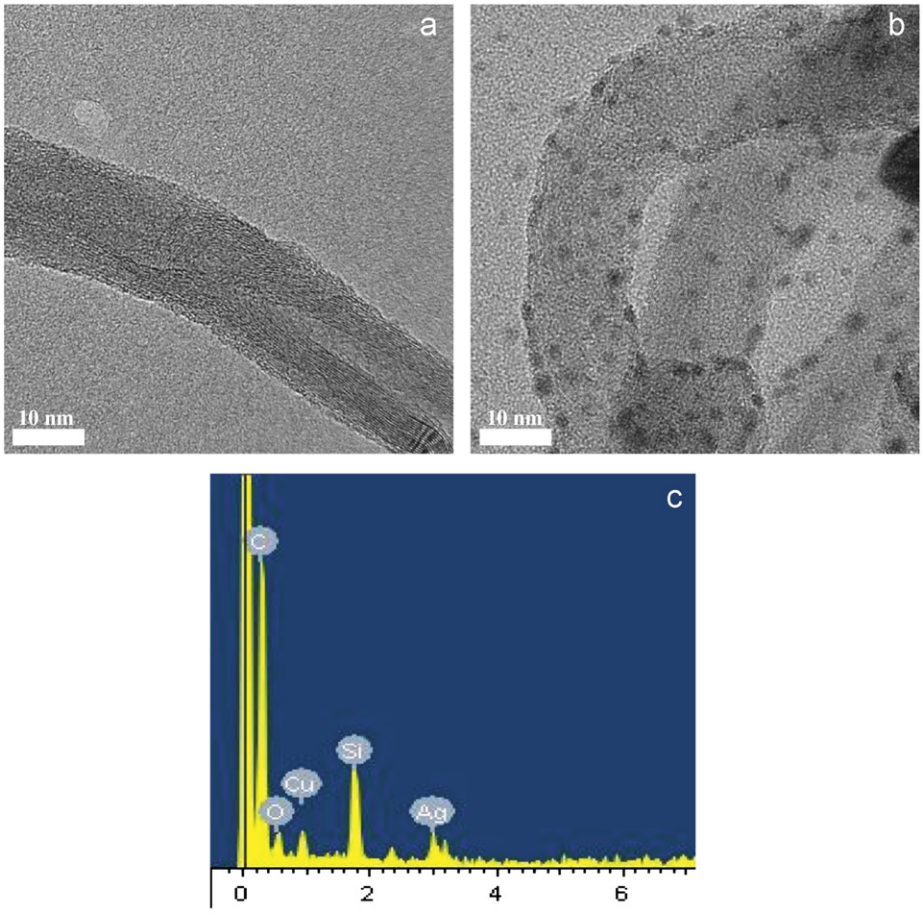

Fig. 2. TEM images of (a) pristine MWNTs, (b) Ag-MWNTs, and (c) EDX image of Ag-MWNTs.

3.2. Characterization of Ag-MWNTs/PANI

Fig. 4 shows the FT-IR spectra of MWNTs, A-MWNTs, Ag-MWNTs, and Ag-MWNTs/PANI. There are no characteristic peaks for pristine MWNTs. In oxidized MWNTs, the appearance of a broadband at 3400 cm^{-1} and absorbance at 1720 cm^{-1} is, respectively, attributed to hydroxyl groups and carbonyl groups on the surface of the oxidized MWNTs, resulting from the functionalization of the MWNTs. However, the relative intensity of the peak at 1720 cm^{-1} in the Ag-MWNTs is lower than in A-MWNTs, indicating the decrease of electron density of the carboxyl (C═O) oxygen atom, probably due to the interaction between silver nitrate and the C═O group of the A-MWNTs [20]. In Ag-MWNTs/PANI, the bands around 1560 and 1480 cm^{-1} are characteristic stretching bands of nitrogen quinoid (N═Q═N) and benzenoid (N–B–N), resulting from the conducting state of the polymer. The 1290 and 1240 cm^{-1} bands are assigned to the bending vibrations of N–H and asymmetric C–N stretching modes of polaron structure of PANI, respectively. The prominent absorption band around 1120 cm^{-1} (C–N stretching) is due to the charge delocalization over the polymeric backbone [21].

Fig. 5 shows the TGA thermogram of Ag-MWNTs, PANI, and Ag-MWNTs/PANI composites. The Ag-MWNTs reveal a partial loss of about 5% at about 580 °C and then remained till 850 °C. The PANI and Ag-MWNTs/PANI exhibit a total loss of about 54% and 43% at about 600 °C, respectively. These results indicate that the PANI content per gram of the composite is about 38% from the loss of the composites (43%) and Ag-MWNTs (5%) and the Ag-MWNTs content is 62% [22,23]. The thermal degradation of the PANI and Ag-MWNTs/PANI shows a three-step weight loss process, as can be seen in Fig. 5. The first weight loss at around 100 °C is attributed to the loss of water and the weight loss from 220 to 310 °C resulted from the elimination of HCl as dopant. The third weight loss from about 400 to 600 °C corresponds to the thermal decomposition of PANI [24].

Fig. 6 shows the XRD patterns of PANI and Ag-MWNTs/PANI. In pure PANI, two broad peaks can be observed at $2\theta = 20^{\circ}$ and 25°, resulting from the periodicity parallel and perpendicular to the polymer chain [25]. The XRD pattern of the Ag-MWNTs/PANI shows the features of both the Ag-MWNTs and PANI due to a hybrid of Ag-MWNTs and PANI by coating.

The images of Ag-MWNTs and the core/shell nanotubes coated by PANI are shown in Fig. 7. The diameter of the Ag-MWNTs is in the range of 20–30 nm (Figs. 2 and 7(a)). Different from the Ag-MWNTs, the Ag-MWNTs/PANI shows rough surface and increased diameter of 50–80 nm (Fig. 7(b)), resulting from the coating of PANI on the MWNTs. It is indicated that average thickness of the PANI layers coated on the MWNTs is about 30 nm. The Ag-MWNTs/PANI is further confirmed by Fig. 7(c) and (d) using SEM and TEM.

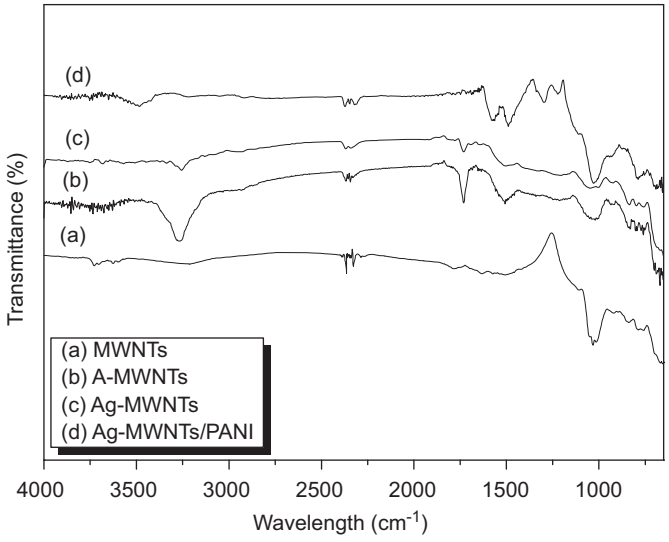

Fig. 4. FT-IR spectra of MWNTs, A-MWNTs, Ag-MWNTs, and Ag-MWNTs/PANI.

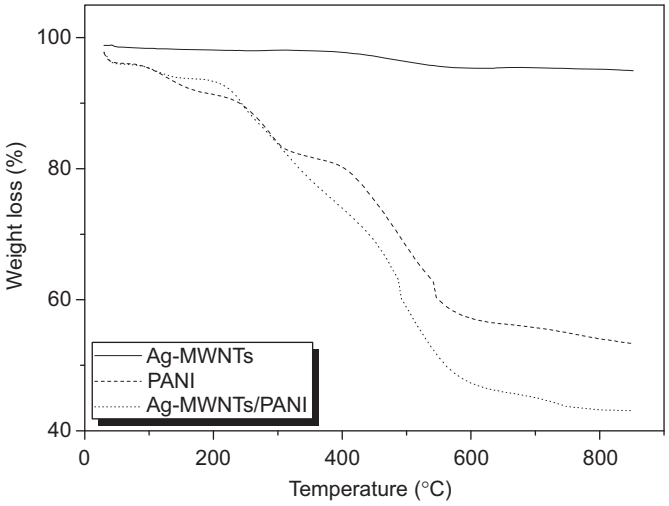

Fig. 5. TGA thermogram of pristine Ag-MWNTs, PANI, and Ag-MWNTs/PANI.

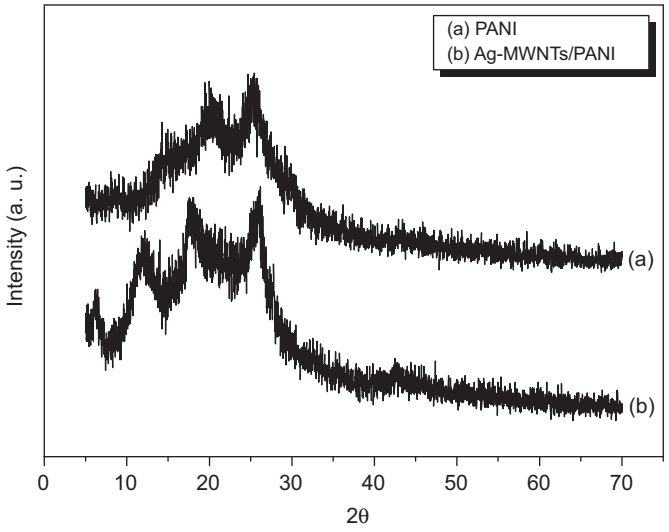

Fig. 6. XRD patterns of PANI and Ag-MWNTs/PANI.

3.3. Electrical conductivity of the Ag-MWNTs/PANI

Fig. 8 shows the electrical conductivity of pure PANI, MWNTs/PANI, and Ag-MWNTs/PANI measured at room temperature. The electrical conductivity of pure PANI prepared without MWNTs is 4.7×10^{-3} S/cm. The MWNTs/PANI (3.4×10^{-2} S/cm) shows increased electrical conductivity with the addition of MWNTs compared with pure PANI. This is attributed to the π–π interaction between the surface of the MWNTs and the quinoid ring of the PANI [26]. In addition, the MWNTs having high electrical conductivity play the role of a conducting bridge in the composites, resulting from the formation of a network structure. Furthermore, the electrical conductivity of the Ag-MWNTs/PANI composites remarkably increases with an increasing Ag concentration. With Ag decoration onto the MWNTs, the electrical conductivity of the Ag-MWNTs/PANI composites increases up to

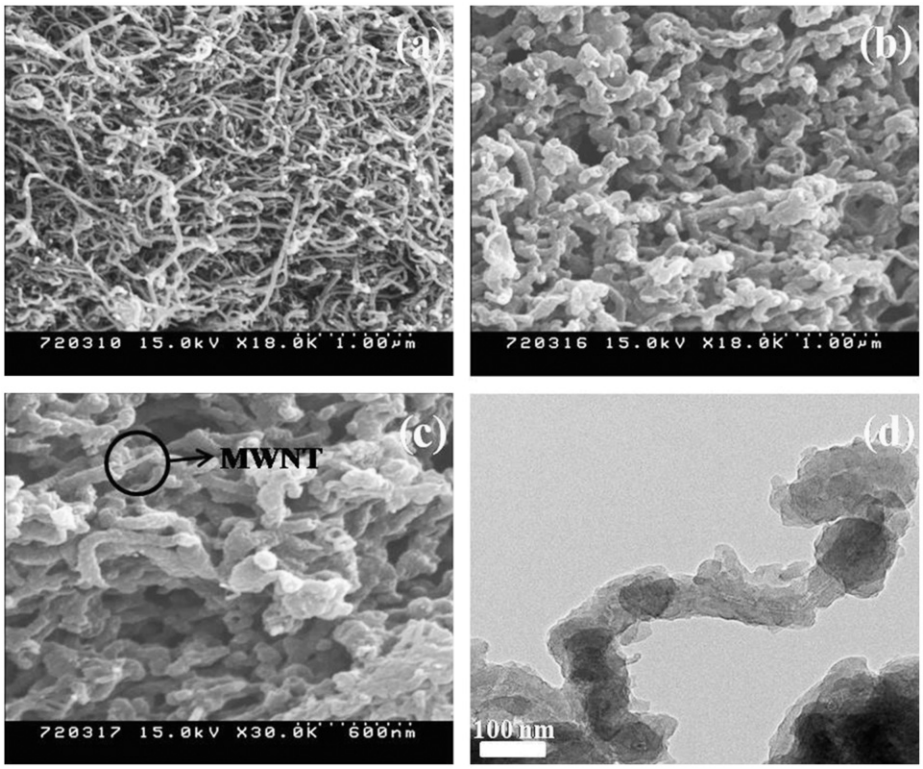

Fig. 7. SEM images of (a) Ag-MWNTs, (b) Ag-MWNTs/PANI, (c) magnified Ag-MWNTs/PANI, and (d) TEM image of Ag-MWNTs/PANI.

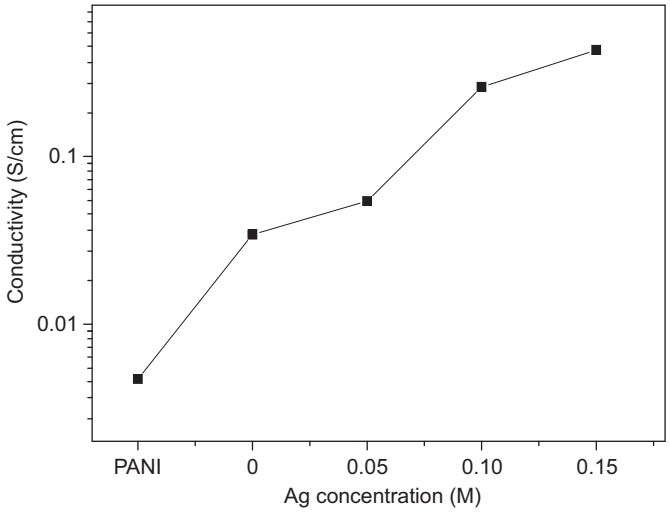

Fig. 8. Electrical conductivity of Ag-MWNT/PANI as a function of Ag concentration.

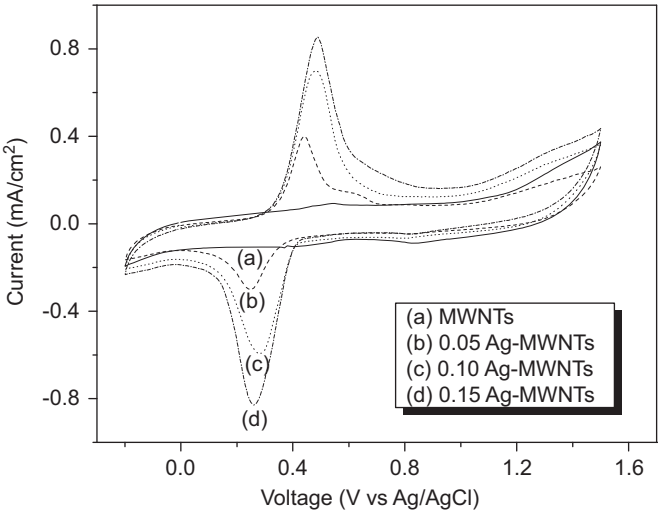

Fig. 9. Cyclic voltammetry of Ag-MWNTs as a function of Ag concentration.

about two orders compared with the MWNTs/PANI composites, which resulted from the decrease of the contact resistance between the PANI and MWNTs. As expected, Ag deposited onto MWNTs showed a synergy effect on the electrical conductivity of the MWNTs due to a higher conductivity of Ag ($\sigma = 6.30 \times 10^5$ S/cm) than that of the pristine MWNTs. This indicates that Ag-MWNTs can serve as an effective conducting filler to enhance the electrical conductivity of PANI [27].

3.4. Electrochemical performance of the Ag-MWNTs/PANI

Fig. 9 shows the cyclic voltammogram of the Ag-MWNTs, which was measured in a 1.0 M sulfuric acid solution as an electrolyte. As shown in Fig. 9, the pristine MWNTs exhibited a broad peak and low current density, whereas the Ag-MWNTs had a pair of redox peaks at 0.25 and 0.50 V due to the redox of Ag nanoparticles. In addition, the electrochemical activity and current density increased with an increasing Ag concentration. This shows the Ag-MWNTs had a high activity towards the hydrogen ions. Furthermore, the oxidation peaks of Ag show more shift with an increasing Ag concentration compared to the reduction peaks. This indicates that the oxidation of the Ag-MWNTs occurs more easily than reduction of the Ag-MWNTs [28].

Fig. 10 shows the cyclic voltammogram of the Ag-MWNTs/PANI. To investigate the effect of Ag nanoparticles, electrochemical performance was measured for PANI with pristine MWNTs and Ag-MWNTs. It can be seen that the Ag-MWNTs/PANI composites exhibit a higher broad redox peak and active surface area

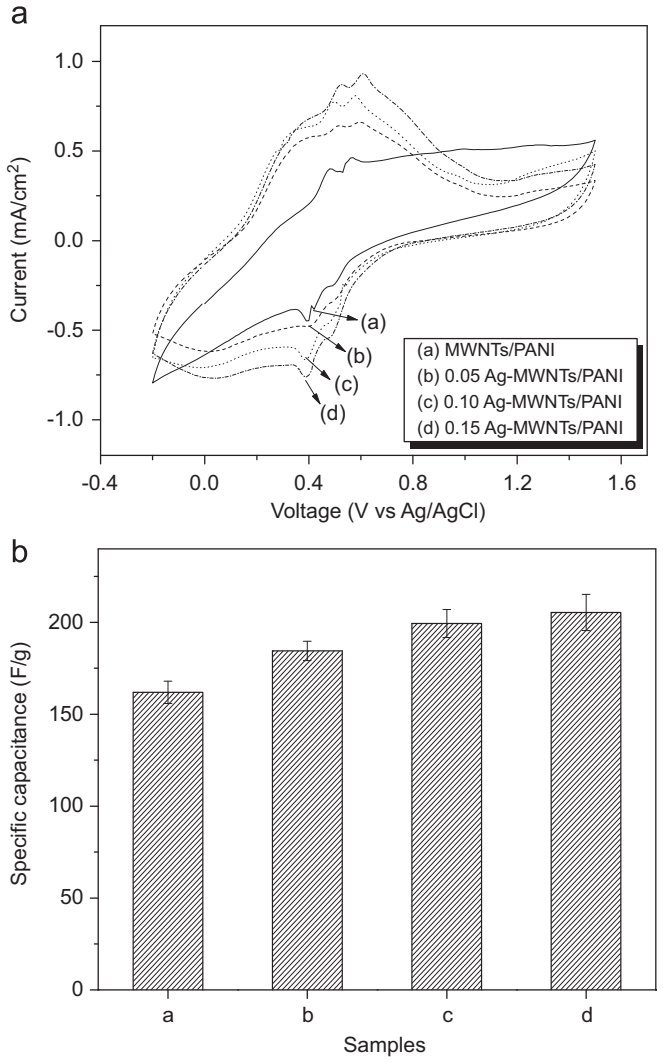

Fig. 10. Cyclic voltammetry (a) and specific capacitance (b) of MWNTs/PANI and Ag-MWNTs/PANI as a function of Ag concentration; a: MWNTs/PANI, b: 0.05 M Ag-MWNTs/PANI, c: 0.1 M Ag-MWNTs/PANI, and d: 0.15 M Ag-MWNTs/PANI.

compared with MWNTs/PANI, indicating a high specific capacitance of the Ag-MWNTs/PANI. In addition, the current density of the Ag-MWNTs/PANI increased remarkably with an increasing Ag concentration, resulting from the electrocatalytic activity of Ag nanoparticles deposited onto MWNTs. These improved electrochemical performances can be explained as follows: (1) Ag nanoparticles provide a bridge effect at the interface between the MWNTs and PANI, and serve as efficient supporting and catalytic materials. This indicates that the Ag nanoparticles could provide a reduction of the contact resistance at the interface between MWNTs and PANI, and the enhanced electrical conductivity of the composites can reduce the energy loss during charge-discharge, leading to an increase in the electrochemical utilization of MWNTs/PANI [29,30], and (2) the presence of the nitrogen groups of the PANI cause a pseudocapacitance reaction, leading to asymmetry of CV curves [31].

From the CV data, the specific capacitance (C_{spec}) for the composite electrodes is shown in Fig. 10(b), and can be calculated as

$$C = \frac{i}{mS} \quad (1)$$

where $S=(\Delta V/\Delta t)$ is the scan rate, i the discharge current, Δt the discharge time corresponding to the voltage difference ΔV, and m the electrode mass. As shown in Fig. 10(b), the specific capacitance of MWNTs/PANI increases with the incorporation of Ag nanoparticles. The highest C_{spec} value (205 F/g) was found with 0.15 M Ag-MWNTs/PANI compared to 162 F/g for MWNTs/PANI, which resulted from the synergistic effect between Ag nanoparticles and MWNTs/PANI [32]. Consequently, the Ag nanoparticles incorporated between the MWNTs and PANI could provide a larger conductive network than MWNTs/PANI. Therefore, core/shell Ag-MWNTs/PANI are favorable for the production of electrode materials and have a superior electrochemical performance to that of conventional MWNTs/PANI electrodes.

4. Conclusions

In this study, the MWNTs were decorated by Ag nanoparticles and the effect of Ag-MWNTs on the electrochemical behavior of Ag-MWNTs/PANI was investigated. It was found that Ag nanoparticles having about 4 nm diameter were deposited onto the MWNTs. The Ag-MWNTs were successfully encapsulated by PANI via oxidation polymerization. The electrical conductivity of the PANI increased remarkably with the addition of MWNTs and Ag-MWNTs. Cyclic voltammetry indicated that the Ag-MWNTs/PANI composites had a higher catalytic activity and active surface area than MWNTs/PANI, which was attributed to the catalytic effect of the Ag nanoparticles deposited onto the MWNTs.

Acknowledgements

This work was supported by INHA University Research Grant and Carbon Valley Development Project of the Ministry of Knowledge Economy, Korea.

References

[1] Z. Spitalsky, D. Tasis, K. Papagelis, C. Galiotis, Prog. Polym. Sci. 35 (2010) 357–401.
[2] W. Bauhofer, J.Z. Kovacs, Compos. Sci. Technol. 69 (2009) 1486–1498.
[3] J.N. Coleman, U. Khan, W.J. Blau, Y.K. Gun'ko, Carbon 44 (2006) 1624–1652.
[4] S.S. Park, S.B. Lee, N.J. Kim, J. Ind. Eng. Chem. 16 (2010) 551–555.
[5] H. Zhang, H.X. Li, H.M. Cheng, J. Phys. Chem. B 110 (2006) 9095–9099.
[6] C. Basavaraja, N.R. Kim, E.A. Jo, R. Pierson, D.S. Huh, Bull. Korean Chem. Soc. 30 (2009) 1543–1546.
[7] R. Sainz, A.M. Benito, M.T. Martinez, J.F. Galindo, J. Sotres, A.M. Bari, B. Coraze, O. Chauvet, W.K. Maser, Adv. Mater. 17 (2005) 278–281.
[8] X. Wang, F. Zhang, X. Zhu, B. Xia, J. Chen, S. Qiu, J. Li, J. Colloid Interface Sci. 337 (2009) 272–277.
[9] Y.Y. Kim, J. Yun, Y.S. Lee, H.I. Kim, Carbon Lett. 12 (2011) 48–52.
[10] E. Zelikman, M. Narkis, A. Siegmann, L. Valentini, J.M. Kenny, Polym. Eng. Sci. 48 (2008) 1872–1877.
[11] Y. Ma, S.H. Ali, L. Wang, P.L. Chiu, R. Mendelsohn, H. He, J. Am. Chem. Soc. 128 (2006) 12064–12065.
[12] V. Georgakilas, P. Dallas, D. Niarchos, N. Boukos, C. Trapalis, Synth. Metals 159 (2009) 632–636.
[13] T. Wu, Y.W. Lin, C.S. Liao, Carbon 43 (2005) 734–740.
[14] V. Selvaraj, M. Alagar, Electrochem. Commun. 9 (2007) 1145–1153.
[15] L. Guo, Z. Peng, Langmuir 24 (2008) 8971–8975.
[16] U. Ugarte, A. Chatelain, W.A. De Heeger, Science 274 (1996) 1897–1899.
[17] P.M. Ajayan, S. Iijima, Nature 361 (1993) 333–334.
[18] R. Kou, Y. Shao, D. Wang, M.H. Engelhard, J.H. Kwak, J. Wang, V.V. Viswanathan, C. Wang, Y. Lin, Y. Wang, I.A. Aksay, J. Liu, Electrochem. Commun. 11 (2009) 954–957.
[19] A. Zamudio, A.L. Elias, J.A. Rodriguez-Manzo, F. Lopez-Urias, G. Rodriguez-Gattomo, F. Lupo, Small 2 (2006) 346–350.
[20] P. Jiang, S.Y. Li, S.S. Xie, Chem. Eur. J. 10 (2004) 4817–4821.
[21] P. Saini, V. Choudhary, B.P. Singh, R.B. Mathur, S.K. Dhawan, Mater. Chem. Phys. 113 (2009) 919–926.
[22] S.P. Armes, S. Gottesfeld, J.G. Beery, F. Garzone, S.F. Agnew, Polymer 32 (1991) 2325–2330.
[23] S. Wang, Z. Tan, Y. Li, L. Sun, T. Zhang, Thermochim. Acta 441 (2006) 191–194.
[24] D. Lee, K. Char, Polym. Degrad. Stabil. 75 (2002) 555–560.
[25] N.R. Chiou, A.J. Epstein, Adv. Mater. 17 (2005) 1679–1683.

[26] T. Jeevananda, Siddaramaiah, N.H. Kim, S.B. Heo, J.H. Lee, Polym. Adv. Technol. 19 (2008) 1754–1762.
[27] P.C. Ma, B.Z. Tang, J.K. Kim, Carbon 46 (2008) 1497–1505.
[28] P. Yang, W. Wei, C. Tao, Anal. Chim. Acta 585 (2007) 331–336.
[29] W. Sun, G. Chen, L. Zhang, Scr. Mater. 59 (2008) 1031–1034.
[30] S. Kim, S.J. Park, Anal. Chim. Acta 619 (2008) 43–48.
[31] K. Kawaguchi, A. Itoh, S. Yagi, H. Oda, J. Power Sources 172 (2007) 481–486.
[32] J. Yan, T. Wei, Z. Fan, W. Qian, M. Zhang, X. Shen, F. Wei, J. Power Sources 195 (2010) 3041–3045.